JOURNAL OF SOLID STATE CHEMISTRY 73, 200–208 (1988)

The Structure, Energetics, and Reactivity of Extended Defects of Copper Oxide

V. A. SADYKOV,* S. F. TIKHOV, G. N. KRYUKOVA,
N. N. BULGAKOV, V. V. POPOVSKII, AND V. N. KOLOMIICHUK

*Institute of Catalysis, Siberian Branch of the USSR Academy of Sciences,
Prospekt Lavrentieva, 5, Novosibirsk 630090, USSR*

Received January 5, 1987; in revised form September 28, 1987

For a discrimination of extended defects of copper oxide in terms of their stability and reactivity a sample of CuO was annealed in the vacuum thermochamber of an electron microscope and in a stream of helium at 200–400°C. The relaxation of the defect structure was studied by electron microscopy and X-ray small-angle scattering. The removal of oxygen from copper oxide was accompanied by rapid disappearance of microstrains. Simultaneously, the development of a dislocation network and the rearrangement of twins enhanced the reactivity of the oxide (the rates of reduction by CO and catalytic oxidation of CO by O_2). Therefore, the active centers of the surface may be associated with dislocations and twins. One of the reasons for high reactivity of such defect centers is that they stabilize the highly reactive weakly bound oxygen.

Introduction

Earlier, by means of electron microscopy, it was shown that the main types of extended defects in copper oxide are twins, dislocations, and microstrains (*1*). However, it remained unclear with which of these defects the active centers of CuO surface are associated. According to (*2*) reactive defects serve as centers of nucleation of Cu_2O and Cu during CuO reduction. Moreover, under sufficiently mild reducing conditions oxygen is easily removed from outlets of the reactive defects on activation of CuO by active zone broadening (*2*, *3*). Imaging of changes in defect structure by electron microscopy during treatment of CuO under mild reducing conditions might resolve this problem. Oxygen bonding energies on oxide surfaces play a dominant role in reactions of complete oxidation (*4*). Thus, a theoretical evaluation by semiempirical interacting bond methods (IBM) (*5*) for the probable structures of adsorption defect centers may provide an independent verification of conclusions concerning defect reactivities.

Since X-ray small-angle scattering (SAS) provides information concerning defects of single crystals (*6*) it seems worthwhile to apply this procedure to our study.

Experimental

In the present paper the same CuO samples as in (*1*–*3*) (Table I) were used. The rates of CuO reduction by CO (1% CO

---

* To whom correspondence should be addressed.

0022-4596/88 $3.00

in He) and CO catalytic oxidation (1% CO and 1% O_2 mixture in He) were determined in a pulse/flow microcatalytic installation using a 1-cm^3 microreactor with a vibrofluidized catalyst bed and a solid electrolyte Pyrex glass (*2*, *4*).

Sample 1 (Table I) was annealed in an electron microscope JEM-100C column under high vacuum (10^{-7} Torr) upon heating up to 400°C and in He at 310 and 400°C. The sample was prepared for the EM investigation as in (*1*).

More complicated experiments consisted of several repeated reductions of CuO-1 by pulses of 1% CO in He, with subsequent reoxidation in oxygen at 400°C (reduction–oxidation cycles). The degree of CuO reduction was limited to ~50% of the oxygen monolayer, thus preventing nucleation of Cu/Cu_2O.

X-ray small-angle scattering experiments were carried out with Cu*Kα* radiation with a nickel filter and by using an amplitude analyzer.

Results

In Situ Electron Microscopy

Figure 1a is an electron micrograph of the initial sample CuO-1. It is characterized by periodically arranged bands 250–500 Å wide, with an alternation in contrast associated with polysynthetic twins (*1*). The boundary between the parts of twins is visible as alternate bright and dark narrow lines.

On raising the temperature to 200°C (Fig. 1b) the shape of the bands corresponding to twins, as well as their width, remains unchanged, while the interface between the twin parts begins to become rearranged. A dislocation network develops on that part of the crystal free of twins.

Further heating to 300°C (Fig. 1c) enhances the contrast of bands: they become somewhat narrower (180–450 Å) and the twin boundaries appear as single lines. The diffraction pattern (see the top inset in Fig. 1c) becomes symmetric (spots are compa-

TABLE I

STRUCTURAL PROPERTIES OF CuO SAMPLES ACCORDING TO ELECTRON MICROSCOPY AND SMALL-ANGLE SCATTERING DATA

					SAS (Å)	
No.	Sample	$S_{specific}$ (m^2/g)	Morphology	Peculiarites of crystalline structure	Main maxima	Mean diameter of inhomogeneities
1	CuO-1 nitrate	0.5	Platelet thickness 500 Å	Monocrystals	15; 60	28.6
2	CuO-2 nitrate	0.4	Platelets with well-developed faces 0.1–1.5 μ	Lattice parameter is increased; crystals textured with the size of blocks of ~300 Å, angle of misorientation ~3°; monocrystalline particles	19; 90	28.7
3	"Wire"	0.1	Platelets with well-developed faces 0.01–0.1 μ and up to 3 μ	Textured crystallites, block ~200 Å, angle of misorientation, ~15–45°	34	34.6
4	Hydroxide	8.6	Extended (up to 1 μ) particles 0.1 μ in diameter with rounded platelets 0.2–0.4 μ	Monocrystals	15; 70	24.5
5	Pure for analysis	0.96	Platelets with well-developed faces 0.1–1.5 μ	Monocrystals	19	23.1

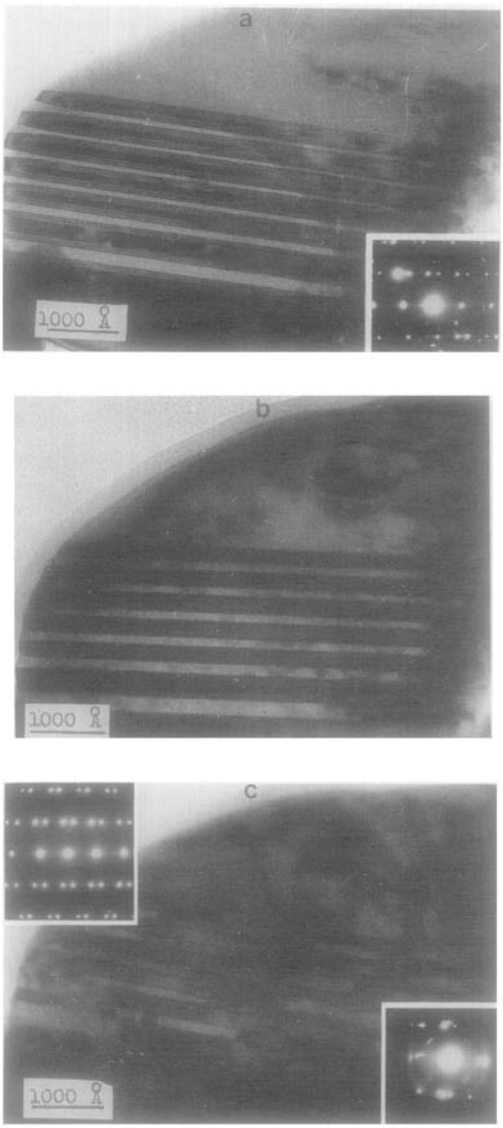

FIG. 1. Image of a CuO particle annealed in the thermochamber of an electron microscope: (a) initial sample; (b) after heating at 200°C; (c) after heating at 300°C.

rable by intensity), indicating the disappearance of dislocations on the twin boundaries. The twinning angle calculated from the figure decreased from 18 to ca. 12°.

On raising the temperature from 300 to 400°C the image contrast of the CuO crystal grows, due to formation of a fairly highly developed dislocation network. As shown by selected area electron diffraction patterns (see the bottom inset in Fig. 1c) the phase composition of this sample corresponds to Cu_2O. After heating to 450° the twins disappear.

Thus, *in situ* heating leads to reduction of CuO, in agreement with previously published results of infrared and X-ray photoelectron spectroscopy (*3*, *7*, *8*). This shows the easy reduction of the surface layer of CuO and of the even more stable copper aluminate by vacuum treatment at 200–400°C. Since annealing of initial CuO at 400°C in air or oxygen did not lead to any variation of defect structure we conclude that the rearrangement of twin structure and the dislocation network development after vacuum treatment was caused by the loss of oxygen.

Annealing in He

In situ investigations have some disadvantages because it is then impossible to study simultaneously the reactivity of CuO with CO. Therefore, experiments were performed on annealing of CuO in He in a microreactor with a vibrofluidized catalyst bed and solid electrolyte Pyrex glass. It was shown that CuO-1 has a low electrode potential stable in oxygen (Table II), comparable to the potential of CuO sample containing Na impurities. It is substantially lower than the potential of pure samples of CuO (~ 0 in O_2 (*2*)). A flame photometry test revealed, however, that the Na content in CuO-1 is less than $10^{-2}\%$; therefore, the low potentials are not due to this admixture. During heating in He an irreversible increase in electrode potential was detected. After 3–4 hr of annealing the electrode potential was close to the values for pure samples of CuO.

Such annealing enhances the initial rates of reduction and catalytic oxidation of CO and somewhat diminishes the "quasi-

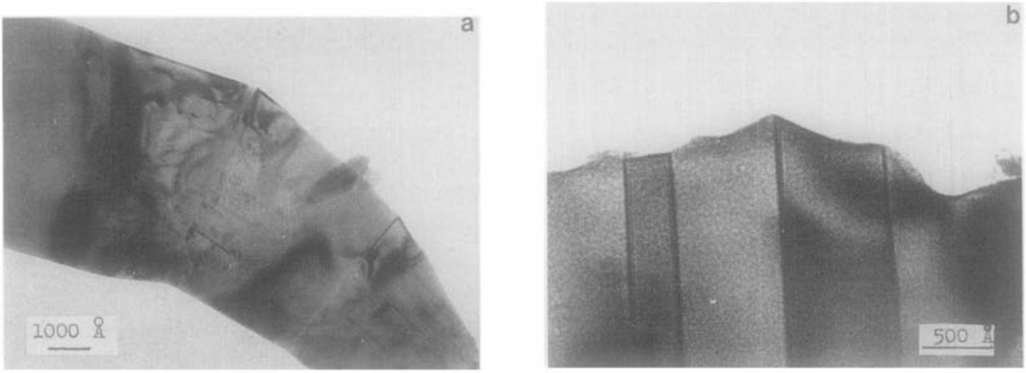

FIG. 2. Micrograph of a CuO-1 particle after annealing in He at 400°C (a) and after several reduction–oxidation cycles (b).

stationary" (after 2 hr in flow of 1% CO + 1% O_2 in He) catalytic activity. Figure 2a presents an electron micrograph of typical CuO particles after annealing in He. Annealing greatly decreases the number of microstrains and leads to the development of a dislocation network and to reconstruction of twin boundaries. After annealing at 400°C in He the twins remained visible, in contrast with the results of the *in situ* treatment, the phase composition corresponding to CuO. Since the pressure of oxygen in He (10^{-3} Torr) is substantially higher than in the chamber of an electron microscope (10^{-7} Torr) the differences may be readily explained by the more oxidative conditions in He.

After several reduction–oxidation cycles a considerable decrease in dislocation density and twin angle and an increase in the distances between twin planes (Fig. 2b) was found. This is accompanied by a decrease in catalytic activity of this sample by 1 to 1.5 orders of magnitude.

X-Ray Small-Angle Scattering

Extended defects, i.e., regions of disordered structure, have an altered electron density and, consequently, a different scattering power of X-rays, as compared to a regular structure. This should give rise to scattering maxima associated with these inhomogeneities (9). In first approximation the data were analyzed as for ordinary par-

TABLE II

INFLUENCE OF ANNEALING ON THE REACTIVITY AND ELECTRODE POTENTIAL OF COPPER OXIDE AT 185°C

Treatment conditions	Initial rate of reduction (10^{17} (CO molec/m^2 · s))	Rate of catalysis (10^{18} (CO molec/m^2 · s))		E (mV)	
		Initial	After 2 hr	O_2	He
Initial sample CuO-1	7.1	6.6	1.8	−570	−1000
Annealed in He for 2 hr at 400°C	9.0	—	—	—	−450
Annealed in He at 310°C, reoxidized in O_2 at 310°C	—	12.0	1.3	−230	−415

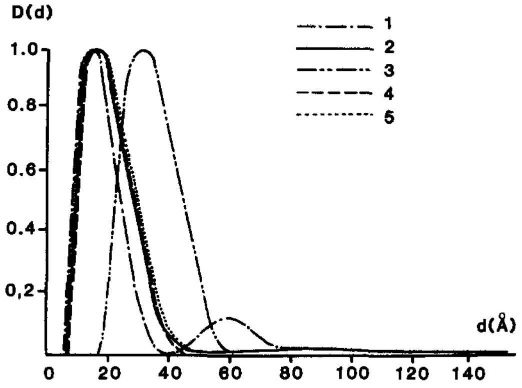

FIG. 3. SAS distribution function for initial samples of CuO. Samples are numbered as in Table I.

ticles for which the size distribution is calculated from the equation:

$$I(h) = \int D(R)m^2(R)i_0(hR)dR,$$

where h is the function of scattering angle $\left(h = 4\frac{\sin\theta}{\lambda}\right)$, λ is the wavelength of radiation used, $I(h)$ is the experimental intensity of scattered radiation, $D(R)$ is the function of size distribution of particles, $i_0(hR)$ is a characteristic function of scattering by an individual particle, and $m(R)$ is an excess number of electrons in a particle as compared to the same volume of environment. We have applied the SAS technique with the aim of qualitatively monitoring changes in the defect structure when passing from one sample of CuO to another. A spherical structure of the inhomogeneities has been used for simplicity. The integral equation $I(h)$ for a set of experimental points is solved with respect to $D(R)$ using a least-squares method. The resulting $D(R)$ are normalized so that the maximum value is equated to 1. Application of SAS has revealed that for all samples the distribution curves have maxima in a rather narrow range 15–80 Å (Table I, Figs. 3 and 4). Such small particles are absent in oxides studied by electron microscopy. Furthermore, the size of blocks, i.e., regions of coherent scattering in polycrystalline particles, does not coincide with the position of SAS maxima. It is therefore assumed that the observed maxima are related to extended defects in CuO. Actually, the change of the defect structure of nitrate–CuO-1 as the result of annealing is accompanied by variations in the distribution function of SAS: the maximum at ~60 Å disappears and that at ~15 Å shifts to the bigger diameters and is widened. In the first approximation it may be supposed that the change of the number of atoms in these inhomogeneities after annealing is proportional to the change of the area under the maximum of SAS curve.

Electron microscopy had shown that after annealing a strong dislocation network began to develop and the twin boundaries rearranged, both types of defects having characteristic dimensions 10–20 Å, corresponding to the maximum in $D(R)$. In addition, after annealing the microstrains with typical diameters of 50–200 Å disappeared. Therefore we conclude that variations of the distribution function after annealing correspond to a change in the number of

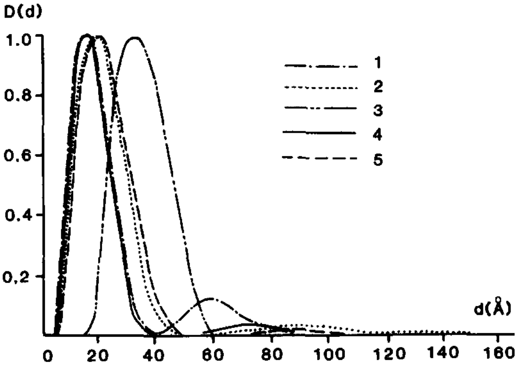

FIG. 4. Change of SAS distribution function after the treatment of CuO sample: 1, sample 1; 2, sample 1 after annealing in He at 310°C; 3, sample 3; 4 and 5, sample 3 after annealing in the reaction mixture 1% CO + 4% O_2 between 185–310°C, up to a steady-state activity; results of two separate experiments with prolonged exposure in the reaction mixture for curve 4.

atoms included in the extended defects. The qualitative agreement in the changes of the defect structure after annealing, as revealed by both methods, allow one to postulate that the maximum of the distribution function at small diameters is attributable to dislocations and twin interfaces and for larger diameters is associated with microstrains. Such attribution clarifies the change in the SAS distribution function when passing from one sample to another (Table I, Fig. 3). That is, samples composed of single-crystal particles (hydroxide, nitrate 1) with twins and dislocations as predominant defects, which are limited in their dimensions, have a narrow maximum in the SAS distribution function. Samples with block structure (nitrate 2, "wire") with large angles of misorientation between blocks have rather large regions of disorder in their interblock boundaries. This leads to a wide maximum in distribution functions shifted toward larger diameters.

Discussion

1. Reactivity of Defects

It was found that extended defects are rather reactive, rearranging their structure under mild reduction. Since for ideal blocks of CuO the surface oxygen is bound with sufficient strength (the heat of adsorption of O_2 ca. 240 kJ/mole (*10*)) its removal from regular sites by vacuum treatment is quite unlikely. Therefore, the easy loss of oxygen from CuO in these conditions may be explained as arising from the low binding energy of oxygen at positions of emergence of extended defects. Because in complete oxidation the weakly bound oxygen is the most reactive, the emergence points of the extended defects may play the role of active centers. This is in agreement with the fact that a narrowing of the maximum of SAS for "wire" CuO, resulting from a prolonged treatment in the reaction mixture (i.e., the decrease of the number of centers bound with extended defects), is accompanied by a fall in the rate of CO catalytic oxidation by ~2 orders of magnitude and by a loss of topochemical reduction of CuO by carbon monoxide (*11*). The decrease in density of extended defects in CuO-1 after the reduction–oxidation cycles also led to a decrease in catalytic activity. Therefore one may correlate the density of the twin boundaries and dislocations with the reactivity of CuO. The active centers of copper oxide surface are thus probably associated with these extended defects.

Annealing of sample 1 revealed no lowering of reactivity with decreasing concentration of microstrains. One may conclude that active centers of CO oxidation are not connected with these defects. At the same time the increase of *E* with annealing points to the fact that low values of electrode potential are due to defects of this type.

2. Analysis of the State of CuO Surface at the Intersection with Extended Defects

Oxidized surface. A discrimination of extended defects by means of reactivity allows one to determine the reasons for the high activity of centers bound with them. As a first step the most developed CuO faces should be determined. According to (*1*) these are generally the (010), (001), and (101) faces. Moreover, extinction contours at the edges of the image of CuO platelets and a lower density of the image of these edges indicate changes in their thickness, probably along (110) and $(\bar{1}\bar{1}0)$ diagonal faces.

In most cases the state of oxygen in the oxidized CuO surface at the sites of intersection with extended defects is the same as for ideal CuO. The M_2O form of oxygen, with the adsorption heat ~240 kJ/mole, predominates, while only negligible amounts of highly reactive MO form, with an adsorption heat ~39 kJ/mole (*5, 10*). Additional centers of stabilization in the

*M*O form of oxygen may exist on the dislocation step on (001) planes.

The second center for adsorption of oxygen as MO units may be associated with the intersection of the (001) twin with the diagonal $(\bar{1}\bar{1}0)$ face. Here oxygen is in nearly square planar coordination with copper atoms (Fig. 5) and does not possess high reactivity. However, it creates steric hindrances to adsorption as M_2O on four copper atoms whereas adsorption as *M*O is quite possible.

Thus on the oxidized surface of CuO the sites for stabilization of weakly bound oxygen may be associated with dislocations and twins.

Reduced surface. It has been shown that treatment of CuO in He enhances its reactivity. According to (*12, 13*) the activation was also observed after gentle reduction of CuO with H_2. This may simply be due to an increase in the number of defect centers as the result of the development of a dislocation network. Yet it may possibly be due to the rearrangement of the above-mentioned structure of extended defects.

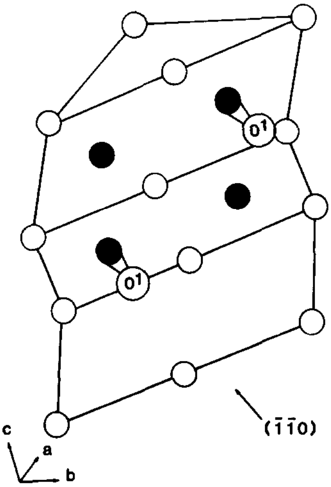

FIG. 5. Adsorption of oxygen in *M*O form at the intersection of a (001) twin with the $(\bar{1}\bar{1}0)$ face of CuO. Large open circles correspond to oxygen atoms, small filled circles to Cu atoms.

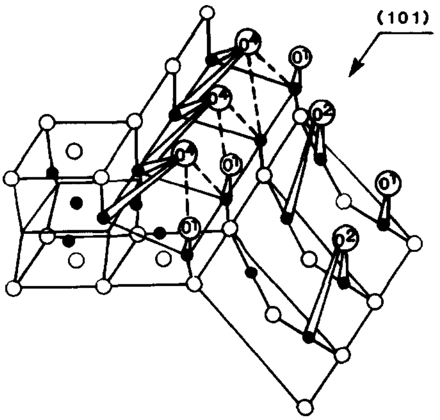

FIG. 6. Structure of completely reduced (001) twin and its intersection with the (101) face of CuO.

The analysis by IBM of various possible types of relaxation of Cu atoms in the reduced (001) twin has revealed the energetically most probable structure (shown in Fig. 6). After oxygen removal the Cu atoms should return to their normal position in the CuO configuration. Then the copper planes should approach each other by 0.5 Å along **c** and should be shifted relative to each other along **a** by 0.34 Å. This yields a symmetric structure of the twin interface (there are two Cu–Cu distances of ca. 2.65 Å and two of 3.09 Å) and leads to the formation of three new Cu–Cu bonds for every removed oxygen atom. The enthalpy of this reconstruction is ca. −60 kJ/g atom. As a result the entire process of oxygen removal from (001) twin with formation of the structure described above requires only 380 kJ/g atom of oxygen (oxygen is converted to a free atom). This value is substantially lower as compared to ~440 kJ/g atom of oxygen necessary for oxygen removal, followed by formation of an isolated oxygen vacancy in the bulk of CuO. The calculation has also revealed that CuO crystals with reduced (001) twins did not disproportionate to CuO and Cu phases since this process will increase enthalpy by ca. 2.1 kJ/mole. Changes in entropy *S* will evidently be negative upon disproportionation and thus would not compensate for an energetically unfavorable process.

The reduction of (100) twins with an appropriate rearrangement creates only one additional Cu–Cu bond for every removed oxygen atom. For this case the enthalpy of oxygen removal is higher (~420 kJ/g atom of oxygen) and the reduction of the (100) twin is less probable. The oxygen in the core of dislocations may be highly mobile owing to the distorted coordinations of atoms (*14*). This explains the easy loss of oxygen from their vicinity once a dislocation network has formed under reducing conditions.

Dislocations as well as microstrains on the twin boundaries disappeared after the reducing treatment of CuO. This may be explained by the absence of abnormally short Cu–Cu distances for the symmetric configuration in the vicinity of reduced (001) twin planes.

Consider a step on the (101) face formed by reduced (001) twin (Fig. 6). Each Cu atom at the base of the step is bound with six copper and one oxygen atoms; each one at the top is bound with two oxygen and six copper atoms. Therefore, oxygen from the gas phase will first be adsorbed on more unsaturated sites at the base. It should be bound with 2 Cu atoms from the bottom; however, binding with 1 or 2 copper atoms from the top is also possible. This oxygen will produce steric hindrances for the formation of the M_2O configuration on copper atoms at the top of the step. At the same time these atoms remain accessible to the adsorption of oxygen as MO with a heat of adsorption 12 kJ/mole, as calculated by IBM. This value is considerably lower than 39 kJ/mole on regular copper atoms. However, the most important feature here is not the decrease of binding energy but the increase of the number of adsorption centers.

Since the MO form of oxygen is removed from active centers in a weakly reducing medium or on contact of the oxidized sample with CO at room temperature, the above defects provide Cu^{1+} sites for adsorption of CO. Clustering of Cu ions at the intersection of defects with the surface will lead to a lower frequency of vibration ν_{CO} (*3*) for CO adsorbed on defect centers in comparison with CO adsorbed on regular sites. This implies that a weakly bound, and consequently more reactive, CO can be stabilized on defect centers; this may be one of the reasons for the high activity for carbon monoxide catalytic oxidation.

Reoxidation of CuO after reduction should inevitably lead to incorporation of oxygen in interstitial positions with a tetrahedral configuration of surrounding Cu atoms. At temperatures of oxidation lower than the temperature of preparation the reoxidation will be incomplete, thus preserving the defect structure in the vicinity of the twin planes. As a result gentle reoxidation only partly deactivates prereduced CuO (*12, 13*). At higher temperatures of the oxidation the process will be complete, and the distances between copper atoms in habit plane should increase to the values corresponding to normal CuO structure; also, the twins will disappear. This model may explain the decrease of the density of twin boundaries after completion of cycles of CuO reduction followed by reoxidation at 400°C.

References

1. G. N. KRYUKOVA, V. I. ZAIKOVSKII, V. A. SADYKOV, S. F. TIKHOV, V. V. POPOVSKII, AND N. N. BULGAKOV, *J. Solid State Chem.* **73,** 191 (1988).
2. V. A. SADYKOV, S. F. TIKHOV, V. V. POPOVSKII, AND G. N. KRYUKOVA, *Kinet. Katal.* **26,** 168 (1985).
3. YU. A. LOKHOV, V. A. SADYKOV, S. F. TIKHOV, AND V. V. POPOVSKII, *Kinet. Katal.* **26,** 177 (1985).
4. G. K. BORESKOV, *in* "Catalysis: Science and Technology," Vol. 3, p. 39, Springer-Verlag, Berlin/Heidelberg/New York (1982).
5. N. N. BULGAKOV, V. YU. ALEKSANDROV, AND

V. V. Popovskii, *React. Kinet. Catal. Lett.* **4**, 1473 (1976).

6. H. H. Atkinson and P. B. Hirsch, *Philos. Mag.* **3**, 213 (1958).
7. G. Ertl, R. Hierl, H. Knözinger, N. Thiele, and H. P. Urbach, *Appl. Surf. Sci.* **5**, 49 (1980).
8. G. I. Salomatin, L. I. Lafer, and V. I. Yakerson, *Izv. Akad. Nauk SSSR, Ser. Khim.* **8**, 1445 (1979).
9. A. Guinier and G. Fournet, "Small-Angle Scattering of X-Rays," Chapman & Hall, New York (1955).
10. J.-P. Joly, *J. Chim. Phys. Phys. Chim. Biol.* **72**, 1018 (1975).
11. V. A. Sadykov, S. F. Tikhov, and V. V. Popovskii, *Kinet. Katal.* **27**, 147 (1986).
12. A. J. van Dillen and K. P. Geus, *J. Chim. Phys.* **78**, 979 (1981).
13. J. v.-d. Berg and A. J. v. Dillen, *et al.*, *in* "Surface Properties and Catalysis by Non-Metals" (J. P. Bonnete, B. Delmon, and E. Derouane, Eds.), Reidel, Dordrecht (1983).
14. J. Friedel, "Les Dislocations," Gauthiers-Villar, Paris (1956).